

RESEARCH ARTICLE

Curcumin prevents osteocyte apoptosis by inhibiting M1-type macrophage polarization in mice model of glucocorticoid-associated osteonecrosis of the femoral head

Shengyang Jin  | Chunqing Meng | Yu He | Xiaohong Wang | Qimin Zhang | Ze Wang | Wei Huang | Hong Wang

Department of Orthopaedics, Union Hospital, Tongji Medical College, Huazhong University of Science and Technology, Wuhan, 430022, China

Correspondence

Wei Huang and Hong Wang, Department of Orthopaedics, Union Hospital, Tongji Medical College, Huazhong University of Science and Technology, No. 1277 Jiefang Avenue, Wuhan, 430022 Hubei, China.

Email: drhuangwei@126.com (WH) and wanghwh@126.com (HW)

Funding information

National Natural Science Foundation of China, Grant/Award Number: 81672166

Abstract

Inflammation is a contributing factor in osteocyte apoptosis, which is strongly associated with the development of glucocorticoid-associated osteonecrosis of the femoral head (GA-ONFH). Curcumin is a naturally derived drug that regulates immunity and inhibits inflammation. This study aimed to examine the capacity of curcumin to prevent osteocyte apoptosis and GA-ONFH, while elucidating possible mechanisms of action. C57/BL6 female mice were divided into control, GA-ONFH, and curcumin-treated GA-ONFH groups. We determined the effect of curcumin on the polarization of RAW264.7 and the apoptosis of MLO-Y4 cells. We found that curcumin reduced the infiltration of M1-type macrophages in the femoral heads and alleviated systemic inflammation in GA-ONFH models. Additionally, curcumin decreased the apoptosis of osteocytes in the femoral heads and the ratio of GA-ONFH in mice. Further, *in vitro* curcumin intervention inhibited M1-type polarization via the Janus kinase1/2-signal transducer and activator of transcription protein1 (JAK1/2-STAT1) pathway. Taken together, this study demonstrates that curcumin is effective in preventing osteocyte apoptosis and the development of GA-ONFH in a mouse model. Curcumin prevents inflammatory-mediated apoptosis of osteocytes in part through inhibition of M1 polarization through the JAK1/2-STAT1 pathway. These findings provide novel insights as well as a potential preventive agent for GA-ONFH. This article is protected by copyright. All rights reserved.

KEYWORDS

apoptosis, curcumin, glucocorticoid-associated osteonecrosis of the femoral head (GA-ONFH), macrophages, osteocyte

1 | INTRODUCTION

Femoral head necrosis is a disease that is associated with high rates of disability. The clinical course is progressive, resulting in the eventual

collapse of the necrotic area in the femoral head, and subsequent hip dysfunction in most patients.¹ Glucocorticoid-associated osteonecrosis of the femoral head (GA-ONFH) accounts for a large proportion of non-traumatic femoral head necrosis.² GA-ONFH commonly develops

This is an open access article under the terms of the Creative Commons Attribution-NonCommercial-NoDerivs License, which permits use and distribution in any medium, provided the original work is properly cited, the use is non-commercial and no modifications or adaptations are made.

© 2020 The Authors. *Journal of Orthopaedic Research*® published by Wiley Periodicals, Inc. on behalf of Orthopaedic Research Society

in patients receiving short-term, high doses of glucocorticoids or long-term moderate doses. Multiple factors have been implicated in the development of GA-ONFH, and the molecular mechanisms involved remain unclear. Additionally, there are few effective drugs available that effectively prevent or treat the disease at the early stages.³⁻⁵

Recent studies have focused on the vital role that osteocyte apoptosis has in the development of GA-ONFH. Osteocytes comprise more than 95% of the cellular components in bone tissue; thus, normal osteocyte function is crucial for healthy bone development and maintenance as osteocytes release a myriad of signaling molecules and cytokines, thereby influencing bone function.^{1,6,7} Osteocyte apoptosis accounts for the initial bone cell death in GA-ONFH patients, with osteocyte viability being significantly reduced in the femoral head.^{1,8} Apoptosis of osteocytes can act to disrupt the mechanosensory function of the osteocyte network causing a cumulative and irreversible defect, resulting in the initiation of events that cause the collapse of the femoral head.^{1,6,7} Furthermore, masses of apoptotic osteocytes were identified in femoral heads, which were removed during total hip replacement surgeries for GA-ONFH; whereas osteocyte apoptosis was not observed in femoral heads obtained from patients with traumatic osteonecrosis, suggesting that osteocyte apoptosis plays a vital role in the development of GA-ONFH, specifically.^{1,3,9}

Inflammation has also been described as being highly associated with the induction of osteocyte apoptosis.¹⁰ The expression of proinflammatory cytokines, such as tumor necrosis factor- α (TNF- α), were upregulated in the bone marrow and serum of GA-ONFH patients as well as in animal models of disease.¹¹ These cytokines disturb bone homeostasis causing osteocyte apoptosis.¹² Specific macrophage phenotypes have been identified as one of the primary sources of these proinflammatory cytokines. Macrophages polarize into either the M1 proinflammatory phenotype or the anti-inflammatory M2 phenotype.^{13,14} CD86 is an M1 marker, while CD206 is primarily expressed by M2 cells.¹⁵ These two phenotypes do not form mutually exclusive populations but rather tend to coexist. The resulting proportions of each phenotype are dependent on the tissue environment and the balance of activating and inhibitory signals.¹⁶ The M1-M2 dichotomy not only serves to simplify the functional classification of macrophages but also informs the expected inflammatory outcome.^{17,18} If a significant proportion of local femoral head macrophages polarized to the M1 phenotype, upregulation of proinflammatory mediators, including TNF- α and interleukin-1 β (IL-1 β), would occur,^{15,19} which may promote osteocyte apoptosis.¹⁰ In the present study, we, therefore, focused on elucidating the relationship between inflammation and apoptosis of osteocytes as well as its subsequent influence on the development of GA-ONFH.

Curcumin (C₂₁H₂₀O₆) is the primary ingredient in turmeric and has long been employed in the treatment of the inflammatory condition.^{3,20} Previous studies have demonstrated that curcumin regulates immunity and reduces inflammation, and have suggested that it interacts with a myriad of molecular targets involved in the regulation of inflammation.^{3,21,22} We were specifically interested in the anti-inflammatory effect elicited by curcumin and its subsequent impact on osteocyte apoptosis in the early stages of GA-ONFH. Considering that the skeletal system of mice is similar to that of humans,^{23,24} we used a

mouse model of GA-ONFH and demonstrated that curcumin administration attenuates the inflammatory response by interfering with the polarization of M1 macrophages. Our in vitro study revealed that curcumin intervention inhibits macrophage polarization toward M1 and suppresses inflammation via the Janus kinase (JAK)-signal transducer and activator of transcription (STAT) pathway, thereby further reducing inflammation-mediated apoptosis of osteocytes. Thus, the administration of curcumin may serve as an effective preventative agent for GA-ONFH by reducing the apoptosis of osteocytes in the femoral head.

2 | MATERIALS AND METHODS

2.1 | Animal grouping and drug administration

We performed experiments on a total of 72 healthy C57/BL6 female mice, aged 5 to 7 weeks and weighing 20 to 22 g. Animals were purchased from Hubei Provincial Center for Disease Control and Prevention (Wuhan, China). All mice had free access to food and water and were housed in an environment with appropriate light intensity and humidity for 7 days before the administration of treatment. The mice were randomly divided into three groups (n = 24 per group): control group A, model group B, and curcumin intervention group C. The mice in B and C were intraperitoneally (IP) injected with lipopolysaccharide (L2630-10MG; LPS, 20 μ g/kg; Sigma, Shanghai, China) for two consecutive days, followed by intramuscular (IM) injection with methylprednisolone (MPS; 40 mg/kg/d) beginning on the 3rd day.^{24,25} The control were injected with equal volumes of phosphate-buffered saline (PBS). During the treatment period, the height of the feeding troughs was raised, which forced the mice to stand to obtain food. Moreover, the mice were transferred to a rotating cage to encourage running for 2 hours every day. All animals were injected by IM with 30 000 U penicillin per week to prevent infection. Curcumin (C2302; purity >97.0%, TCI Company, Shanghai, China) was suspended with 1% carboxymethylcellulose (CMC, C104984; Sunshine M&E Equipment Co, Ltd, Shanghai, China). Beginning on the 1st day of the experiment, mice in C were administered with curcumin (100 mg/kg) by gavage once per day. Alternatively, mice in A and B were administered with equivoluminal 1% CMC by gavage once a day. In each group, three mice were randomly sacrificed on weeks 0, 1, 2, 3, and 4, and heart blood was extracted. Moreover, after week 4, mice were euthanized under anesthesia to obtain femoral head tissue from each group.

The study was conducted in accordance with the guidance offered in the Guide for the Care and Use of Laboratory Animals (2018). All animal experiments were conducted following protocols approved by the Animal Experimentation Committee of Hubei Provincial Center for Disease Control and Prevention (Wuhan, China).

2.2 | Cell cultures, induction, and intervention

MLO-Y4 and RAW264.7 cells were obtained from Procell Life Science & Technology Co, Ltd. (Wuhan, China). MLO-Y4 and RAW264.7 cells were

cultured in Dulbecco's Modified Eagle's Medium (DMEM, Gibco) supplemented with 10% FBS containing 1% penicillin-streptomycin solution (Sigma, Shanghai, China). Cells were incubated at 37°C with saturated humidity and a 5% CO₂ atmosphere. After achieving approximately 80% confluency, cells were passaged and selected for further experiments. RAW264.7 cells were then cultured with media containing LPS (100 ng/mL) and interferon-gamma (IFN- γ , 315-05; 2.5 ng/mL; Peprotech, Suzhou, China) for 12 hours to induce polarization. Different concentrations of curcumin (0, 6.25, 12.5, and 25 μ mol/L) were added to the RAW264.7 cultures; these groups were designated as group MI, group 6.25 MI, group 12.5 MI, and group 25 MI, respectively. Untreated RAW264.7 cells were used as control, which was designated as the group RAW.

Once MLO-Y4 cells reached logarithmic growth, they were added to 6-well plates at 4×10^5 cells/well and incubated with conditioned media (CM) from the different RAW264.7 culturing groups (RAW, MI, 6.25 MI, 12.5 MI, and 25 MI) at 37°C with saturated humidity and 5% CO₂ atmosphere. The rate of osteocyte apoptosis was detected at 6, 12, 24, 48, and 72 hours.

As control, we used different concentrations of curcumin (0, 6.25, 12.5, and 25 μ mol/L, designated as group 0, group 6.25, group 12.5, and group 25, respectively) to intervene MLO-Y4 cells and detect the apoptosis rates at 6, 12, 24, 48, and 72 hours.

2.3 | Histological analysis

Femoral head samples were obtained and fixed in phosphate buffer solution (PBS) containing 4% paraformaldehyde and decalcified with 10% ethylenediaminetetraacetic acid (EDTA) solution. The samples were then dehydrated, embedded in paraffin, and cut into 4 μ m thick sections. The sections were stained with haematoxylin and eosin. Histologically, the femoral head was considered necrotic at the early stage when at least one of the following three signs was present: bone marrow cell necrosis, empty lacunae or pycnotic nuclei of osteocytes, or any evidence of repair such as the presence of granulation tissue, fibrosis, or appositional bone formation.²⁶ Meanwhile, the histopathology is characterized by the presence of sparse or fragmented trabeculae and disorganization of tissue.²⁴

In this study, osteonecrosis was mainly evaluated by three independent researchers, based on the diffuse presence of empty lacunae or pycnotic nuclei of osteocytes in the bone trabeculae. The ratio of empty lacunae and the ratio of pycnotic nuclei of osteocytes were calculated for each femoral head using a coronal section taken at the maximal femoral width.²⁶

2.4 | Immunofluorescence assay

The sections were treated with rat anti-F4/80 (Ab6640; 1:50; Abcam, Shanghai, China), mouse anti-CD86 (NBP2-44515, 1:50; Novus, Shanghai, China), and rabbit anti-CD206 (Ab195191, 1:50; Abcam) primary antibodies (15 hours, 4°C) followed by staining with Cy3-labeled goat anti-rat

IgG (Bs-0293G-CY3; 1:100, Bioss, Beijing, China), FITC-labeled goat anti-mouse IgG (BA1101, 1:100; Boster Biological Technology Co, Ltd, Wuhan, China), and FITC-labeled goat anti-rabbit IgG (BA1105, 1:10; Boster Biological Technology Co, Ltd) secondary antibodies (1 hour, 20°C), respectively. The sections were then treated with 4,6-diamino-2-phenylindole (DAPI, C1002; Beyotime Biotechnology Co Ltd, Wuhan, China) to stain the nuclei (5 minutes, 20°C). The proportion of M1 and M2 macrophages was evaluated using the mean optical density (MOD) as determined by the ImageJ analysis software.

2.5 | Western blot analysis

Total proteins from the macrophages obtained from the *in vitro* experiments were extracted with radioimmunoprecipitation assay lysis buffer (P0013B; Beyotime Biotechnology Co Ltd) containing phenylmethanesulfonylfluoride fluoride (PMSF, ST506; Beyotime Biotechnology Co, Ltd) for 30 minutes. The total proteins were also eluted from the culture supernatants. Total protein concentration was measured using a Bicinchoninic Acid (BCA) protein assay kit (P0010; Beyotime Biotechnology Co, Ltd). Equivalent amounts of protein (40 μ g) were then electrophoresed in sodium dodecyl-sulphate-polyacrylamide gel (SDS-PAGE) and transferred onto polyvinylidene difluoride (PVDF) membranes (IPVH00010; EMD Millipore, Billerica, MA). The PVDF membranes were blocked for 2 hours with tris-buffered saline with tween buffer (TBST) containing 5% skim milk nonphosphorylated proteins. Membranes were then soaked in an incubation solution containing rabbit anti-STAT1 polyclonal (10144-2-AP, 1:600; Proteintech Group Inc, Wuhan, China), rabbit anti-p-STAT1 monoclonal (9167; 1:1000; Cell Signaling Technology, Danvers, MA), rabbit anti-JAK1 polyclonal (AF5012; 1:1000; Affinity Biosciences, Cincinnati, OH), rabbit anti-p-JAK1 polyclonal (AF2012, 1:1000; Affinity Biosciences), rabbit anti-JAK2 polyclonal (AF6022, 1:1000; Affinity Biosciences), and rabbit anti-p-JAK2 polyclonal (AF3024, 1:1000; Affinity Biosciences) antibodies, at 4°C overnight. Rabbit GAPDH polyclonal antibody (AB-P-R 001, 1:1000; Xianzhi Biotech, Hangzhou, China) served as a loading control. The following day, membranes were washed with TBST six times for 5 minutes, and incubated with horseradish peroxidase-labeled sheep against rabbit secondary antibodies (BA1054, 1:50 000; Boster Biological Technology, Ltd) at 37°C for 2 hours. These antibodies were detected using electrochemiluminescence detection reagent (EMD Millipore) according to the manufacturer's instructions. The films were scanned, and the BandScan program was used to analyze the grayscale.

2.6 | Enzyme-linked immunosorbent assay for proinflammatory mediators

Peripheral blood from mice in each group was obtained at 0, 1, 2, 3, and 4 weeks. Additionally, macrophages were collected from each *in vitro* cell group and the supernatants were collected by centrifugation (225g for 5 minutes) for enzyme-linked immunosorbent assay (ELISA) analysis. The levels of TNF- α and IL- β were quantified using ELISA kits according to the

manufacturer's instructions (E-EL-M0049c, E-EL-M0037c, E-EL-M0044c, respectively; Elabscience Biotechnology Co, Ltd, Wuhan, China).

2.7 | Flow cytometric analysis

Flow cytometry was used to detect the ratio of M1 and M2, and the rate of osteocyte apoptosis. Macrophages and MLO-Y4 cells were collected from in vitro cell group, centrifuged at 225g for 3 minutes, and the supernatants were discarded. Cells were resuspended in PBS to a cell density of 10^6 /mL. One hundred microliters from each cell suspension were added into a flow tube. The cells were then centrifuged at 225g for 3 minutes and washed twice with PBS containing 0.5% bovine serum albumin (Gibco). To detect the ratio of M1 to M2 cells, we added 1 μ g of F4/80-PE (565410; BD Biosciences, Beijing, China) and 1 μ g of CD86-FITC (sc-19617; SANTA) as markers of M1 cells, and 1 μ g of F4/80-PE with 0.25 μ g CD206-APC (17-2061-80; Invitrogen) as markers of M2 cells. The cells were then incubated in the dark for 30 minutes at 4°C. The rate of apoptosis in MLO-Y4 cells was detected by following the instructions of Annexin V-APC/7-AAD Apoptosis Detection Kit (YDQ962; Yuduobio, Shanghai, China). The cells were analyzed using a flow cytometer (FACSCalibur; BD Biosciences). The negative control (NC) group was not treated with antibodies.

2.8 | Statistical analysis

The data were presented as the mean \pm standard deviation (SD). GraphPad Prism 7.04 (GraphPad Software Inc, CA) was used to conduct paired Student *t*-tests and one-way analysis of variance (ANOVA). The differences between rates were tested by χ^2 or Fisher's exact tests, if appropriate. A $P < .05$ was considered statistically significant. All samples were assayed in triplicate in three mice of each group, and all experiments were repeated at least three times.

3 | RESULTS

3.1 | Curcumin inhibited osteocyte apoptosis and alleviated osteonecrosis in a mouse model

As shown in Figure 1A-C, the trabeculae of subchondral bones in B collapsed and became more sparse, slender and disordered than in A, with bone resorption (Figure 1B2) observed. Alternatively, the trabeculae of subchondral bone in C were more organized and denser compared to mice in B. Moreover, the number of nucleus pycnosis of osteocytes and empty lacunae were found to be significantly higher in B compared to A and C (Figure 1D,E). Throughout the study, no mice naturally died in A, two mice died in B (at day 4 and day 23), and two mice died in C (at day 5 and day 13).

Further, as Figure 1F indicates, the incidence of GA-ONFH at 4th week was 0% in A (0/12), 80% in B (8/10), and 30% in C (3/10). These results suggest that our modeling method is effective at inducing

GA-ONFH and that curcumin administration serves to significantly reduce the rate of osteocyte apoptosis in a mouse model at the early stage.

3.2 | Curcumin reduced M1 infiltration in femoral heads and proinflammatory mediators in peripheral blood

Immunofluorescence analysis was used to evaluate the number of macrophages in the bone marrows of femoral heads. As depicted in Figures 2A and 2D, a small number of M1 cells were found in the bone marrow of A. However, the quantity of M1 cells significantly increased in B compared to A ($n = 10$; $P = .0007$); and the quantity of M1 cells decreased in C compared to B ($n = 10$, $P = .0014$). Meanwhile, the quantity of F4/80 and CD206 in these groups did not differ significantly (Figures 2A-C and 2E), suggesting that no obvious changes occurred in the total number of macrophages or the level of M2 infiltration in the femoral head bone marrow.

Further, the secretion of TNF- α and IL-1 β increased with time in B (Figure 2F,G). At the 4-week time point, the concentrations of TNF- α and IL-1 β were significantly higher in B than in A ($n = 3$; $P < .0001$ and $P < .0001$, respectively); whereas the expression levels of the cytokines were seen to be lower in C compared to B ($n = 3$; $P < .0001$ and $P < .0001$, respectively). These results suggested that the secretion of proinflammatory mediators by M1 increased in the GA-ONFH models and that curcumin administration serves to attenuate the inflammatory responses.

3.3 | Curcumin regulated macrophage polarization and significantly inhibited M1 polarization in vitro

In RAW264.7 cultures, 11.97% \pm 0.52% of cells expressed F4/80 and CD86, whereas 44.19% \pm 1.52% of cells expressed F4/80 and CD206. Treatment with LPS and IFN- γ increased the ratio of F4/80 and CD86 positive cells to 55.06% \pm 1.91% ($n = 3$; $P < .0001$), and decreased the ratio of F4/80 and CD206 positive cells to 11.22% \pm 0.5687% ($n = 3$, $P < .0001$; Figure 3A-D). These results suggest that M1 and M2 are not mutually exclusive but rather coexist in RAW264.7 cell cultures. Furthermore, LPS and IFN- γ functioned to induce polarization of RAW264.7 to the M1 phenotype. Following administration of curcumin, the ratio of F4/80 and CD86 positive cells decreased compared to the MI, and the effect became more evident as the concentration of curcumin increased (6.25 MI [$n = 3$, $P = .0133$], 12.5 MI [$n = 3$, $P = .0002$], and 25 MI [$n = 3$, $P < .001$]) (Figure 3A,B). Meanwhile, low doses of curcumin intervention (6.25 μ mol/L) had no significant effect on polarization of M2 cells ($n = 3$; $P = .8565$), however, higher concentrations in the 12.5 MI and 25 MI acted to promote M2 polarization ($n = 3$; $P < .0001$ and $P = .0002$, respectively) as shown in Figure 3C,D. These results indicate that curcumin regulated macrophage polarization, with a particularly significant effect observed against the polarization of M1 cells.

As shown in Figure 3E,F, the levels of secreted TNF- α and IL-1 β were significantly upregulated in the MI compared to that of the RAW ($n = 3$;

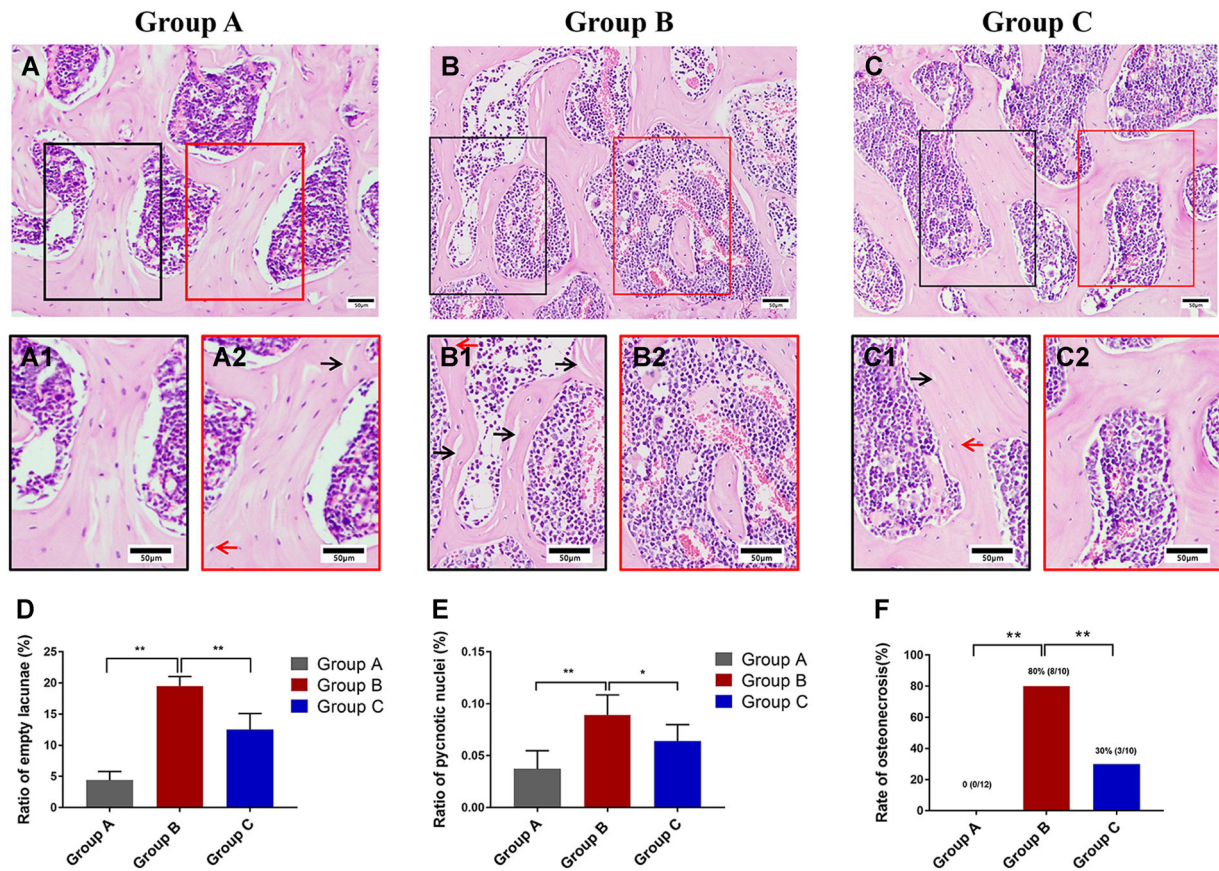


FIGURE 1 A-C, Haematoxylin and eosin staining. The red arrows indicate nucleus pycnosis of osteocytes and the black arrows indicate empty lacunae. D, The proportion of empty lacunae within the femoral head. E, The proportion of nucleus pycnosis of osteocytes within the femoral head. F, The incidence of GA-ONFH in each study group. Data represent the mean \pm SD. Significant differences between the two groups are indicated as * $P < .05$ and ** $P < .01$. GA-ONFH, glucocorticoid-associated osteonecrosis of the femoral head [Color figure can be viewed at wileyonlinelibrary.com]

$P < .001$ and $P < .001$, respectively). Alternatively, the levels of TNF- α and IL-1 β were significantly down-regulated in the 6.25 MI compared to the MI ($n = 3$; $P = .0012$ and $P < .001$, respectively), and this effect became more prominent as the concentration of curcumin increased. These results were consistent with the previous results and further indicated that curcumin acted to inhibit M1 macrophage polarization.

3.4 | Curcumin reduces osteocyte apoptosis induced by macrophages

The rate of apoptosis in osteocytes after treatment with the CM of MI was significantly higher than that observed following treatment with the CM of RAW at 12, 24, 48, and 72 hours ($n = 3$; $P < .0001$, $P = .0001$, $P < .0001$, and $P < .0001$, respectively; Figure 4C-G).

The rates of osteocyte apoptosis following treatment with the CM from 6.25 MI were significantly reduced compared to that in the MI at 48 h and 72 h ($n = 3$, $P = .0138$ and $.0266$, respectively; Figure 4E-G), and the rates of osteocyte apoptosis in 12.5 MI were significantly reduced compared to that in MI at 24, 48, and 72 hours ($n = 3$; $P = .0006$, $P = .0006$, and $P = .0003$, respectively; Figure 4D-G). Moreover, the rates of osteocyte apoptosis in 25 MI were significantly reduced compared to

that in MI at 12 hours, 24 hours, 48 hours, and 72 hours ($n = 3$; $P < .0001$, $P = .0002$, $P = .0004$, and $P < .0001$, respectively; Figure 4C-G).

Different concentrations of curcumin were used to interfere with osteocytes as control. As shown in Figure 4H-N, different concentrations of curcumin had no significant effect on osteocytes apoptosis within 24 hours. At 48 hours, curcumin at a high dose (25 $\mu\text{mol/L}$) increased the apoptosis rate of osteocytes ($n = 3$; $P < .0001$). At 72 hours, curcumin at a medium dose (12.5 $\mu\text{mol/L}$) began to increase the apoptosis rates ($n = 3$; $P < .0001$). When the apoptosis rates of osteocytes were compared between the group 0 and MI, group 6.25, and 6.25 MI, group 12.5 and 12.5 MI, group 25 and 25 MI, we found that the apoptosis rates of osteocytes were significantly lower in curcumin intervention groups than those in conditioned medium intervention groups (except the comparison between group 25 and 25 MI at 6 hours; Figure 4O-R). These results suggest that the CM from MI cultures promoted osteocyte apoptosis, whereas curcumin intervention could inhibit this process. The preventive effect of curcumin on osteocyte apoptosis is indirect through macrophages. Within a certain range, the higher the concentration of curcumin, the longer the time, the more the preventive effect of the drug can be reflected.

More relevant flow cytometric analysis results (6 hours, 12 hours, 24 hours, and 72 hours) can be seen in Figures S6 and S7.

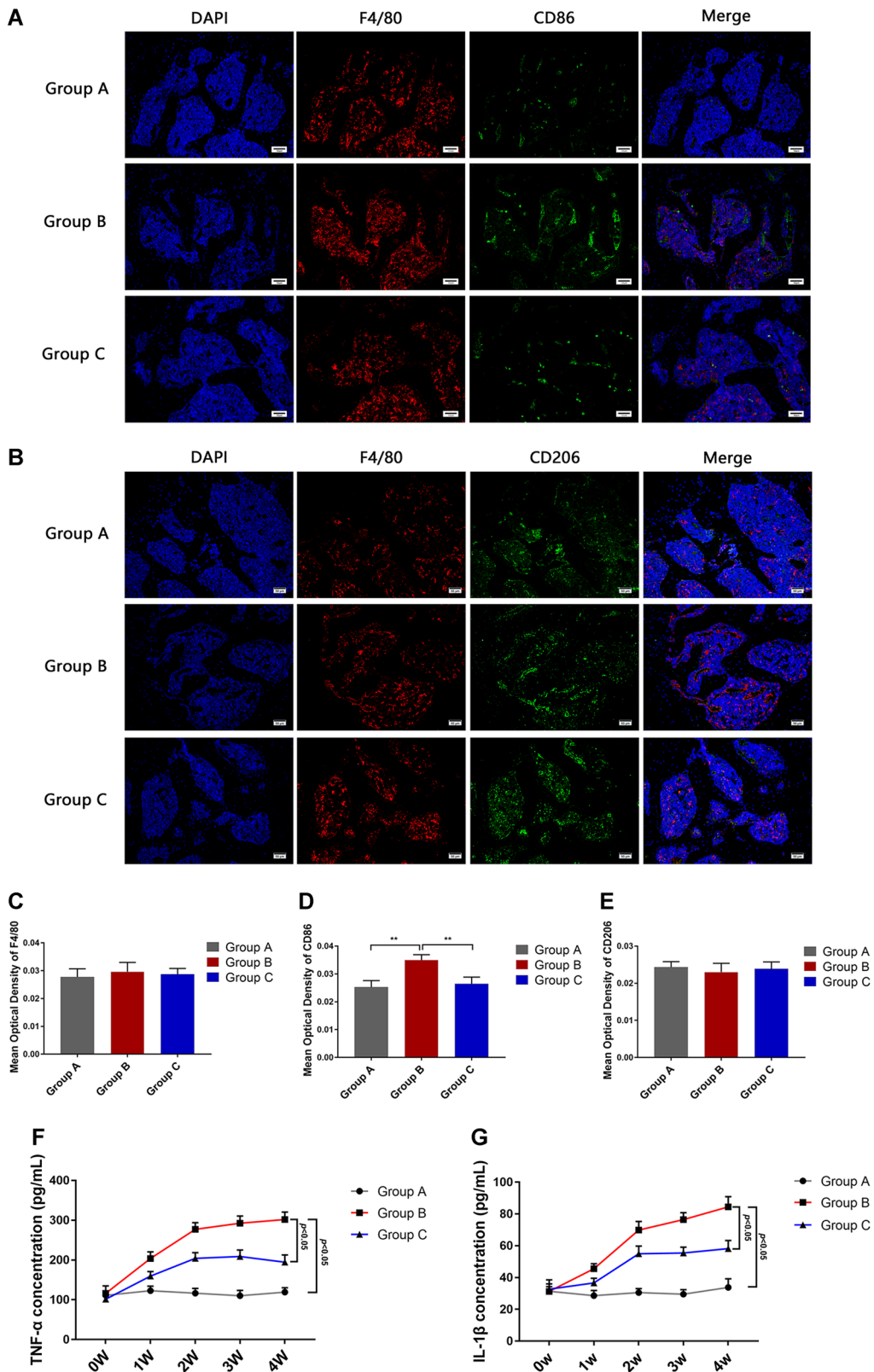


FIGURE 2 A, Immunofluorescence assay for F4/80 and CD86 stained macrophages in group A, B, and C at 4th week. B, Immunofluorescence assay for F4/80 and CD206 stained macrophages in groups A-C at 4 weeks. C-E, Statistical analysis depicting the mean optical density (MOD) of specific indicators in different study groups. F, Levels of TNF- α in the peripheral blood at weeks 0, 1, 2, 3, and 4 in group A, B, and C. G, Levels of IL-1 β in the peripheral blood at weeks 0, 1, 2, 3, and 4 in groups A-C. Data represent the mean \pm SD. * P < .05 and ** P < .01 compared with MI. IL-1 β , interleukin-1 β ; TNF- α , tumor necrosis factor-alpha [Color figure can be viewed at wileyonlinelibrary.com]

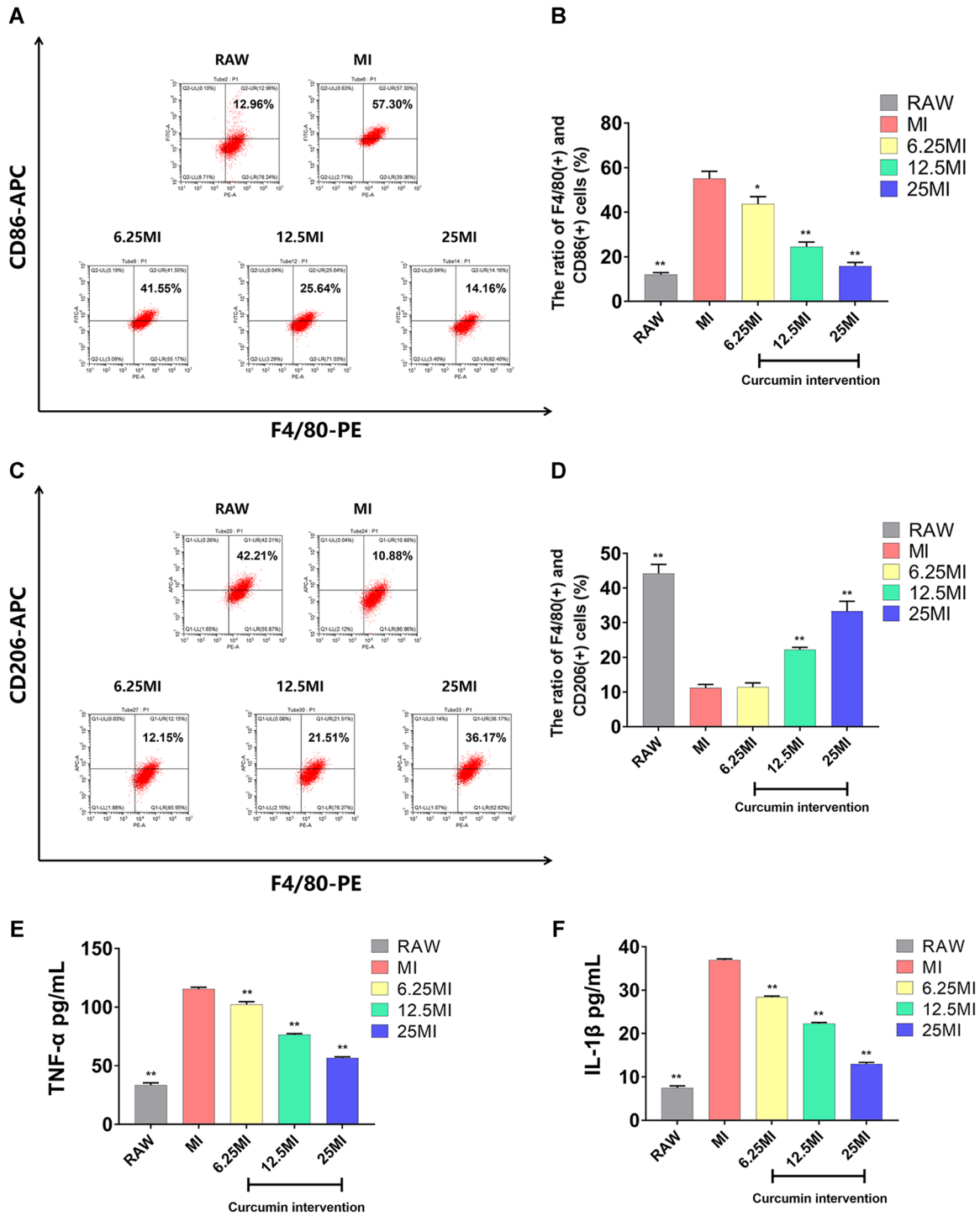


FIGURE 3 A,C, Flow cytometric analysis of surface antigens on macrophages. B,D, Statistical depiction of the percentage of F4/80+CD86+ and F4/80+CD206+ cells in the different study groups. E,F, The level of TNF- α and IL- β in conditioned media (CM) of each group as determined by ELISA. The data are expressed as the mean \pm SD of three independent experiments. * $P < .05$ and ** $P < .01$ compared with MI. ELISA, enzyme-linked immunosorbent assay; IL-1 β , interleukin-1 β ; TNF- α , tumor necrosis factor-alpha [Color figure can be viewed at wileyonlinelibrary.com]

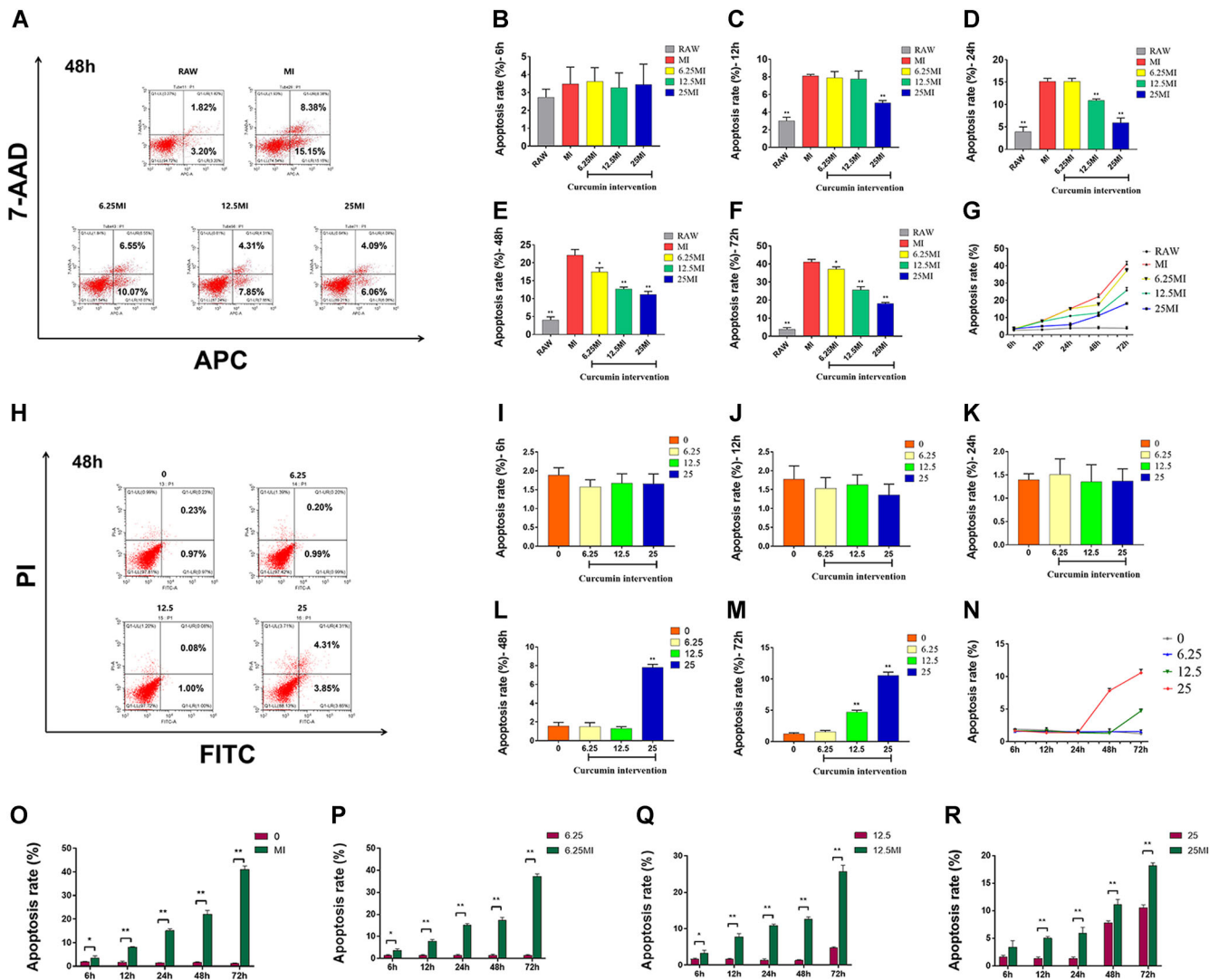


FIGURE 4 A, Representative figure of flow cytometric analysis of osteocyte apoptosis after 48 hours of intervention with CM from each group. B-G, Quantitative analysis of osteocyte apoptosis after 6, 12, 24, 48, and 72 hours intervention with CM from each group. H, Representative figure of flow cytometric analysis of osteocyte apoptosis after 48 hours of intervention with different concentrations of curcumin. I-N, Quantitative analysis of osteocyte apoptosis after 6, 12, 24, 48, and 72 hours intervention with different concentrations of curcumin. O-R, Comparative analysis of the effects of CM from each group and different concentrations of curcumin on osteocyte apoptosis. The data are expressed as the mean ± SD of three independent experiments. **P* < .05, and ***P* < .01 compared with MI (B-F); **P* < .05 and ***P* < .01 compared with group 0 (I-M). CM, conditioned medium [Color figure can be viewed at wileyonlinelibrary.com]

3.5 | Curcumin may inhibit the JAK1/2-STAT1 signaling pathway

The JAK-STAT pathway is vital in promoting the polarization of macrophages towards the M1 phenotype.^{27,28} As shown in Figures 5D-F and 5J-I, the levels of p-JAK1, p-JAK2, and p-STAT1 in MI were significantly higher compared to those in the RAW (*n* = 3, *P* < .0001, *P* = .0003, and *P* < .0001, respectively). Moreover, the expressions of p-JAK1, p-JAK2, and p-STAT1 in the 6.25 MI were significantly lower than that in the MI (*n* = 3, *P* = .0123, *P* = .0481, and *P* = .0137, respectively). The expression of these proteins was seen to further decrease with the addition of curcumin in a concentration-dependent manner. Significant differences were not observed in the expression of JAK1, JAK2, and STAT1 within each

group (Figures 5A-C and 5G-I). These results confirm that the JAK1/2-STAT1 pathway was activated during M1 polarization of macrophages and that curcumin effectively inhibited this pathway.

We also repeated our in vitro study by using the primary culture of the mice bone marrow derived-macrophages. The conclusions were consistent with the results above, and the experimental process and results can be seen in Figures S8-S10.

4 | DISCUSSION

Our results confirm that immune and inflammatory disorders contribute to the progression of osteonecrosis at the early stage of GA-ONFH.

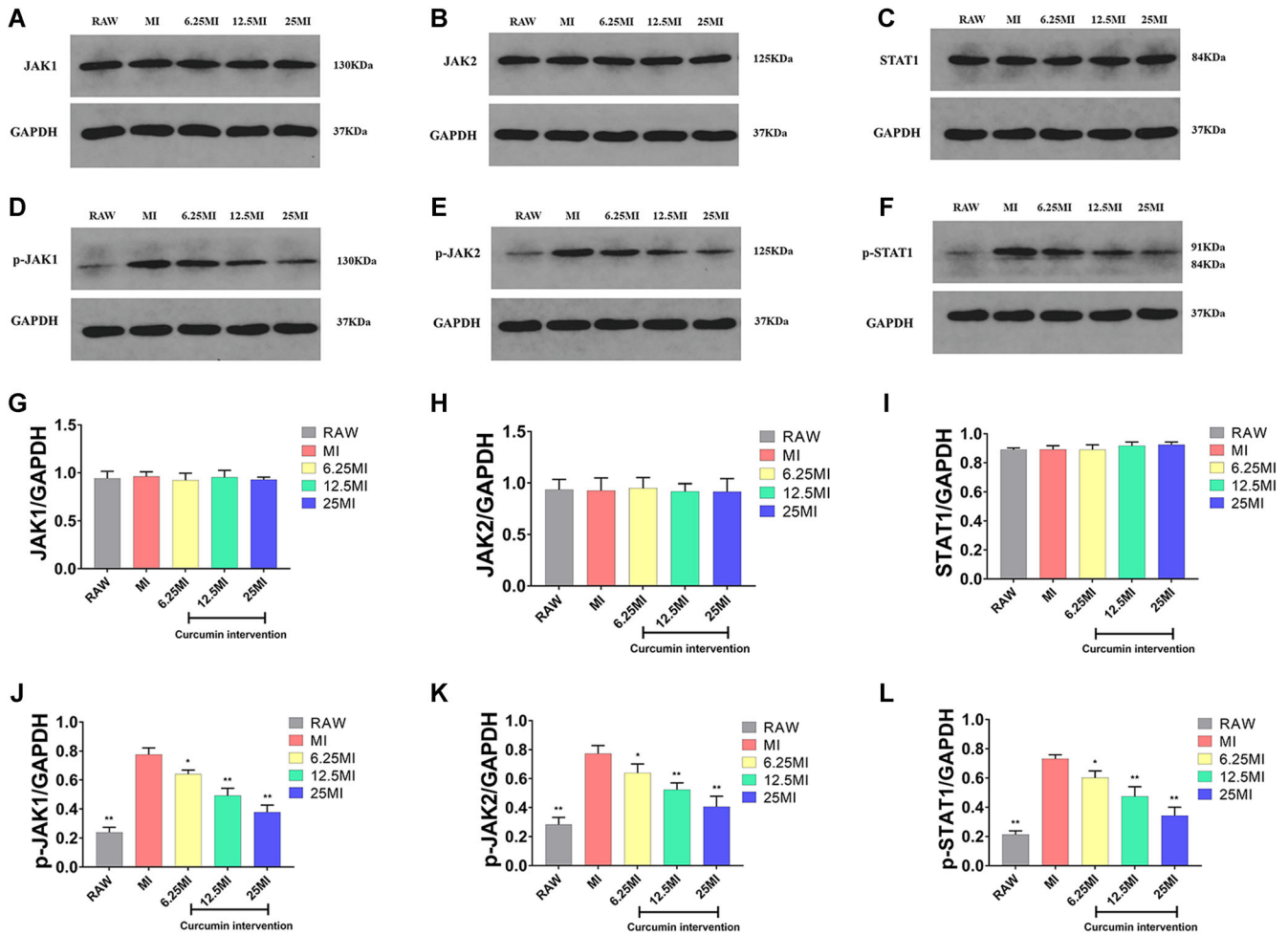


FIGURE 5 A-F, The expression of JAK1, p-JAK1, JAK2, p-JAK2, STAT1, and p-STAT1 in macrophages within each group as determined by western blot analysis. G-I, Quantitative analysis of the bands measured by gray value. The experiment was carried out a minimum of three times, and values are expressed as the mean \pm SD. * $P < .05$ and ** $P < .01$ compared with MI. JAK, Janus kinase; STAT, signal transducer and activator of transcription [Color figure can be viewed at wileyonlinelibrary.com]

Curcumin can play a preventive role in GA-ONFH models by regulating immunity and suppressing inflammation. However, osteonecrosis of the femoral head cannot be entirely prevented by curcumin. Our results (Figure 1) revealed that, although curcumin can effectively reduce the apoptosis of osteocytes and the incidence of GA-ONFH, a portion of the mice in group C developed osteonecrosis. There are several possible reasons to explain the phenomenon.

Firstly, as is mentioned above, GA-ONFH is a disease with complex pathogenesis that is affected by multiple factors, such as cell apoptosis, coagulation abnormalities, aberrant lipid metabolism, oxidative stress, and vasospasm.³⁻⁵ Moreover, many factors have been implicated in the development of osteocyte apoptosis. Osteocyte apoptosis is aggravated by several factors, including the direct effects of glucocorticoids and other indirect factors.^{10,29} Thus, osteonecrosis of the femoral head cannot be entirely prevented by solely regulating the immune response and suppressing inflammation at the early stages of GA-ONFH development.

Secondly, the mechanism by which glucocorticoids cause immune and inflammatory disorders in the early stage of GA-ONFH is complex,

and curcumin cannot reverse the disorders completely. Glucocorticoids are more pleiotropic than previously thought. Glucocorticoids, function as an immune regulator, by priming and strengthening the innate immune system for rapid activation, which promotes inflammation, while also suppressing the adaptive immune system to help restore homeostasis, which has an anti-inflammatory effect.³⁰ Whether the proinflammatory or anti-inflammatory properties dominate depends on many factors, including the dose and time of drug administration, the underlying disease, and the physiological drug target. For example, in the central nervous system, glucocorticoids have been shown to increase the level of inflammation by increasing activation of transcription factors, proinflammatory cytokine expression as well as macrophage extravasation and migration.³¹ In the necrotic sites at the early stage of GA-ONFH, abnormal activation and infiltration of proinflammatory macrophages were identified, and the mechanism may be related to excessive activation of the innate immune system through activation of the TLR4 signaling pathway.^{10,32} As our results show, curcumin, as an immunomodulator, can alleviate inflammation by reducing the infiltration of M1-type

macrophages into the femoral heads in GA-ONFH models, but cannot block the inflammatory response completely. Considering that the mechanism by which glucocorticoids cause macrophage polarization in the early stage of GA-ONFH is complex, and we previously found glucocorticoids alone had little effect on macrophage polarization while using LPS and IFN- γ was a relatively mature method to induce macrophage polarization in vitro experiments, we used LPS and IFN- γ instead of glucocorticoids to induce macrophage polarization. However, the in vivo and in vitro experiments do not match perfectly. So, we will study the mechanism of macrophage polarization in GA-ONFH and make the in vivo and in vitro experiments more compatible in the future study.

In the present study, curcumin was not seen to promote M2 polarization in an animal model, yet in our in vitro study curcumin promoted M2 polarization when the concentration of curcumin was 12.5 or 25 $\mu\text{mol/L}$. However, we did not further examine this phenomenon or the associated mechanism, and thus, cannot say whether this effect contributed to the observed inhibition of the inflammatory response. Besides, curcumin has efficacy in regulating lipid metabolism.^{21,33} Considering that abnormal lipid metabolism is one of the possible mechanisms of GA-ONFH, the preventive effect of curcumin on GA-ONFH may be related to the efficacy in regulating lipid metabolism. These two research directions are meaningful, and we will study in-depth in the future.

Although our findings provide novel insights into the mechanism of GA-ONFH and a potential preventive agent for the disease, however, the translational value of the results in humans needs further evaluation. The small body-weight of mice and their four-legged gait does not accurately mimic the disease process of humans. To compensate for the limitation as best as possible, we raised the height of the feeding troughs, thereby forcing the mice to stand on their hind-quarters to reach their food. Additionally, the mice were transferred to the rotating cage to encourage running for 2 hours every day. By doing so, the mice mimicked human activity as closely as possible. Nevertheless, there will be differences in the pathogenesis of GA-ONFH between mice and humans. Besides, the mice we selected were at puberty and this is a model applied to pediatric osteonecrosis. We did not take it into account that age difference might change the phenotype of the mice and this is a shortcoming of our experiment, which will be improved in our future studies.

In summary, curcumin can reduce inflammatory-induced osteocyte apoptosis and may be an effective preventive agent for GA-ONFH in the early stages. The protective effects of curcumin were mediated, in part, by inhibition of M1 polarization through the JAK1/2-STAT1 signaling pathway. Our findings provide novel insights as well as a potential preventive agent for GA-ONFH. The more elaborate mechanism employed by curcumin to reduce inflammation in GA-ONFH deserves further examination, and the applicability of the results in humans needs further evaluation.

ACKNOWLEDGMENT

This study was supported by the grant 81672166 from the National Natural Science Foundation of China.

CONFLICT OF INTERESTS

The authors declare that there are no conflict of interests.

AUTHOR CONTRIBUTIONS

SJ, WH, and HW contributed to the idea and design of the study. SJ and WH performed the experiments. CM and YH collected the data. XW, QZ, and ZW analyzed the data. SJ drafted the paper. WH substantially revised the paper. HW gave the final approval of the version to be submitted. All authors have read and approved the final manuscript.

ORCID

Shengyang Jin  <http://orcid.org/0000-0001-8803-4974>

REFERENCES

- Weinstein RS, Nicholas RW, Manolagas SC. Apoptosis of osteocytes in glucocorticoid-induced osteonecrosis of the hip. *J Clin Endocrinol Metab.* 2000;85(8):2907-2912.
- Luo P, Gao F, Han J, Sun W, Li Z. The role of autophagy in steroid necrosis of the femoral head: a comprehensive research review. *Int Orthop.* 2018;42(7):1747-1753.
- Weinstein RS. Glucocorticoids, osteocytes, and skeletal fragility: the role of bone vascularity. *Bone.* 2010;46(3):564-570.
- Mont MA, Cherian JJ, Sierra RJ, Jones LC, Lieberman JR. Non-traumatic osteonecrosis of the femoral head: where do we stand today? a ten-year update. *J Bone Joint Surg Am.* 2015;97(19):1604-1627.
- Mankin HJ. Nontraumatic necrosis of bone (osteonecrosis). *N Engl J Med.* 1992;326(22):1473-1479.
- Weinstein RS. Glucocorticoid-induced bone disease. *N Engl J Med.* 2011;365(1):62-70.
- Weinstein RS. Glucocorticoid-induced osteoporosis and osteonecrosis. *Endocrinol Metab Clin North Am.* 2012;41(3):595-611.
- Calder JDF, BATTERY L, Revell PA, Pearse M, Polak JM. Apoptosis—a significant cause of bone cell death in osteonecrosis of the femoral head. *J Bone Joint Surg Br.* 2004;86(8):1209-1213.
- Youm YS, Lee SY, Lee SH. Apoptosis in the osteonecrosis of the femoral head. *Clin Orthop Surg.* 2010;2(4):250-255.
- Wu X, Feng X, He Y, et al. IL-4 administration exerts preventive effects via suppression of underlying inflammation and TNF-alpha-induced apoptosis in steroid-induced osteonecrosis. *Osteoporos Int.* 2016;27(5):1827-1837.
- Fang B, Wang D, Zheng J, et al. Involvement of tumor necrosis factor alpha in steroid-associated osteonecrosis of the femoral head: friend or foe? *Stem Cell Res Ther.* 2019;10(1):5.
- Zhou M, Li S, Pathak JL. Proinflammatory cytokines and osteocytes. *Curr Osteoporos Rep.* 2019;17(3):97-104.
- Martinez FO, Sica A, Mantovani A, Locati M. Macrophage activation and polarization. *Front Biosci.* 2008;13:453-461.
- Mantovani A, Biswas SK, Galdiero MR, Sica A, Locati M. Macrophage plasticity and polarization in tissue repair and remodelling. *J Pathol.* 2013;229(2):176-185.
- Chen S, Lu Z, Wang F, Wang Y. Cathelicidin-WA polarizes *E. coli* K88-induced M1 macrophage to M2-like macrophage in RAW264.7 cells. *Int Immunopharmacol.* 2018;54:52-59.
- Martinez FO, Gordon S. The M1 and M2 paradigm of macrophage activation: time for reassessment. *F1000Prime Rep.* 2014;6:6.
- Saha S, Shalova IN, Biswas SK. Metabolic regulation of macrophage phenotype and function. *Immunol Rev.* 2017;280(1):102-111.
- Loi F, Córdova LA, Pajarinen J, Lin T, Yao Z, Goodman SB. Inflammation, fracture and bone repair. *Bone.* 2016;86:119-130.

19. Mathis D. Immunological goings-on in visceral adipose tissue. *Cell Metab.* 2013;17(6):851-859.
20. Shehzad A, Rehman G, Lee YS. Curcumin in inflammatory diseases. *Biofactors.* 2013;39(1):69-77.
21. Pagano E, Romano B, Izzo AA, Borrelli F. The clinical efficacy of curcumin-containing nutraceuticals: an overview of systematic reviews. *Pharmacol Res.* 2018;134:79-91.
22. Sahebkar A, Cicero AFG, Simental-Mendía LE, Aggarwal BB, Gupta SC. Curcumin downregulates human tumor necrosis factor- α levels: a systematic review and meta-analysis of randomized controlled trials. *Pharmacol Res.* 2016;107:234-242.
23. Ryoo S, Lee S, Jo S, et al. Effect of lipopolysaccharide (LPS) on mouse model of steroid-induced avascular necrosis in the femoral head (ANFH). *J Microbiol Biotechnol.* 2014;24(3):394-400.
24. Xu J, Gong H, Lu S, Deasey MJ, Cui Q. Animal models of steroid-induced osteonecrosis of the femoral head—a comprehensive research review up to 2018. *Int Orthop.* 2018;42(7):1729-1737.
25. Wang B, Yu P, Li T, Bian Y, Weng X. MicroRNA expression in bone marrow mesenchymal stem cells from mice with steroid-induced osteonecrosis of the femoral head. *Mol Med Rep.* 2015;12(5):7447-7454.
26. Zhu H, Cai X, Lin T, Shi Z, Yan S. Low-intensity pulsed ultrasound enhances bone repair in a rabbit model of steroid-associated osteonecrosis. *Clin Orthop Relat Res.* 2015;473(5):1830-1839.
27. Liang YB, Tang H, Chen ZB, et al. Downregulated SOCS1 expression activates the JAK1/STAT1 pathway and promotes polarization of macrophages into M1 type. *Mol Med Rep.* 2017;16(5):6405-6411.
28. Zhang X, Wu J, Ye B, Wang Q, Xie X, Shen H. Protective effect of curcumin on TNBS-induced intestinal inflammation is mediated through the JAK/STAT pathway. *BMC Complement Altern Med.* 2016;16(1):299.
29. Compston J. Glucocorticoid-induced osteoporosis: an update. *Endocrine.* 2018;61(1):7-16.
30. Busillo JM, Cidlowski JA. The five Rs of glucocorticoid action during inflammation: ready, reinforce, repress, resolve, and restore. *Trends Endocrinol Metab.* 2013;24(3):109-119.
31. Sorrells SF, Sapolsky RM. An inflammatory review of glucocorticoid actions in the CNS. *Brain Behav Immun.* 2007;21(3):259-272.
32. Okazaki S, Nishitani Y, Nagoya S, Kaya M, Yamashita T, Matsumoto H. Femoral head osteonecrosis can be caused by disruption of the systemic immune response via the toll-like receptor 4 signalling pathway. *Rheumatology.* 2009;48(3):227-232.
33. Gupta SC, Patchva S, Koh W, Aggarwal BB. Discovery of curcumin, a component of golden spice, and its miraculous biological activities. *Clin Exp Pharmacol Physiol.* 2012;39(3):283-299.

SUPPORTING INFORMATION

Additional supporting information may be found online in the Supporting Information section.

How to cite this article: Jin S, Meng C, He Y, et al. Curcumin prevents osteocyte apoptosis by inhibiting M1-type macrophage polarization in mice model of glucocorticoid-associated osteonecrosis of the femoral head. *J Orthop Res.* 2020;38:2020–2030. <https://doi.org/10.1002/jor.24619>